# SPEED CONTROL OF A MICROPROCESSOR BASED DC DRIVE

## Part I: Design of the Control Loops

Salah Gh. Ramadan, R. Mostafa, and Gamal Sarhan*

## ABSTRACT

The system under consideration is a DC motor drive system consisting of a separately excited DC machine supplied from a DC-chopper and controlled through a microprocessor trainer. In this part of the study, the suitable control loops and their digital controllers are designed. The study is continued in a second part (Part II) of this article where the complete structures of the hardware and the software are discussed.

It is desirable to optimize the efficiency of the overall system and at the same time to obtain a satisfactory transient response of the speed. In the method used, the ratio of the armature current and the field current ($I_a/I_f$) that gives the maximum efficiency of the DC motor is analytically derived and the error term of the current ratio is controlled to be zero at steady state speed of the motor. However at the transient state, the efficiency of the proposed method is not optimal, but the satisfactory transient response is expected in compensation for the non-optimal transient efficiency. This characteristics is desirable, because the instantaneous value of speed is important. On the other hand, the integral value of efficiency is more important than its instantaneous value.

## I. INTRODUCTION

The functional block diagram of studied system is given in Fig.1. The power circuits consist of two DC choppers. The four quadrant DC chopper of the armature circuit consists of two MOSFET switches operating at high chopping frequency, and two darlington power transistors operating in the continuous current conduction mode. This arrangement represents the optimal utilization of the characteristics of both types of devices; fast switching MOSFET and lower conduction losses transistors. Also this arrangement decreases the cost to much. The field circuit consists of a single MOSFET switch constructing one quadrant DC chopper.

In a previous paper [4] the complete design of the two power circuits was designed including selection of the devices, calculation of the power losses and the heat sink requirements. The overall efficiency and its dependence on the load current, the load voltage, the supply voltage and the operating frequency was also established. The active protective means for all devices against the harmful conditions were implemented. The study is continued in

* Dr. Ing. Salah Gh. Ramadan and Gamal Sarhan
  Shoubra Faculty of Engineering, Cairo - Egypt
* Dr. Ramadan Mostafa
  Military Technical College, Cairo - Egypt

the present paper where the control circuits are designed to get optimal efficiency. In the second paper (Part II) the complete design of the software and the hardware is given and the experimental results of the whole system are illustrated.
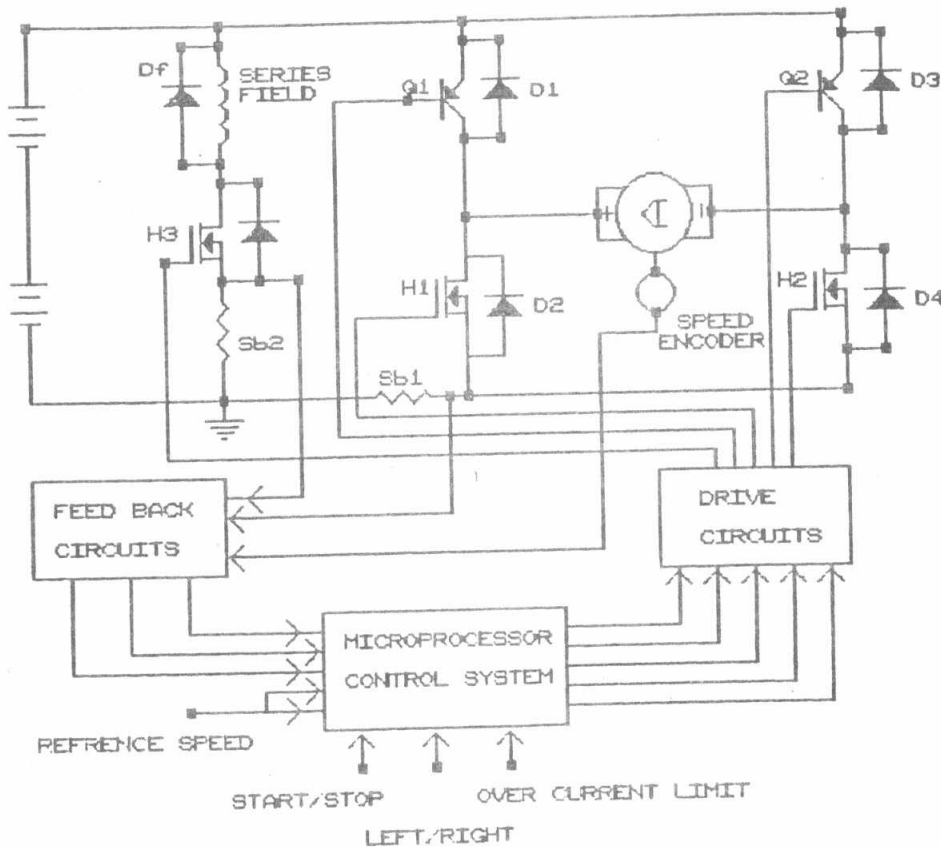


Fig.1 The Function Block Diagram of the Drive System

## II. THE ANALYSIS OF THE CONTROL SYSTEM

As stated above. in the present work, it is desirable to optimize the efficiency of a DC drive and at the same time obtaining a satisfactory transient response of the speed. The motor used is a separately excited DC motor. Until now, this motor has been used in the industrial field when high accurate speed control is necessary over a wide speed range. The possibility of the speed control of the system that gives the optimal efficiency by means of controlling both armature and field currents simultaneously has been proposed in several works. However details of the realization of such systems are not considered. In the following section the losses of the machine are studied to clarify the method of control.

### A. The Consideration of Losses:

Generally, the efficiency of the DC motor system under a given output power $P_0$ is represented by;

$$n = \left[ \frac{P_o}{P_o + P_L + P_m} \right] \tag{1}$$

where:   $P_m$ = mechanical losses
$P_L$ = iron losses + copper losses + stray losses + converter losses

In order to maximize the efficiency (n), the sum of losses must be minimized at the output $P_o$. The mechanical losses $P_m$ are not controllable under condition of a given desired speed. The controllable losses $P_L$ take the following form:

$$P_L = P_a + P_f \tag{2}$$

where:
$P_a$ = power losses associated with armature current including converter losses. These can be approximated with a good accuracy by:

$$P_a = K_a \times I_a^2 \tag{3}$$

To get the best possible value of $K_a$. $P_a$ is determined at several values of $I_a$ and least squares method of approximation is used. $P_f$ is the power losses associated with the field current including the converter losses.

$$P_f = I_f^2 R_f + \text{field converter losses} + P_e + P_h \tag{4}$$

The eddy current $P_e$ and the hysteresis $P_h$ losses can be noted in the following:

$$P_e = K_e n^2 B_m^2 \quad \text{and} \quad P_h = K_h n B_m^{1.6} \tag{5}$$

Since $B_m$ depends on $I_f$. thus $P_f$ is a function of the current $I_f$ and the speed n. If saturation effect is neglected $P_f$ can be approximated with a good degree of accuracy into the following form:

$$P_f = K_f(n) I_f^2 \tag{6}$$

$K_f(n)$ depends on the motor. and usually the linearized value $K_f(N_o)$ at an operating speed $N_o$ is used. Its value is changed at several operating points to cover the wide range of the speed. The suitable values are determined by the same method used to obtain $K_a$ but with the speed as a parameter.

$K_f(N1)$    for speeds up to    1000        rpm.
$K_f(N2)$    for speeds between 1000 and 1500 rpm.
$K_f(N3)$    for speeds between 1500 and 2000 rpm.
$K_f(N4)$    for speeds above    2000        rpm.

Assuming an unsaturated magnetic circuit. the generated torque $T_m$ is given by:
$$T_m = K_T I_a I_f \tag{7}$$

The optimal ratio of $I_a/I_f$. giving the minimum losses under the constant

generated torque at $n = N_o$ is obtained by means of the Lagrange multiplier method. Using Eq.2, the minimum losses are obtained if $dP_L = 0$ where:

$$d P_L = \left[\frac{o\,P_L}{o\,I_a}\right] dI_a + \left[\frac{o\,P_L}{o\,I_f}\right] dI_f \tag{8}$$

Then: $\left[\frac{dI_a}{dI_f}\right] = - \left[\frac{K_f(N_o)I_f}{K_a I_a}\right]$

Since the torque is constant, then from Eq.7, one gets:

$$dT_m = K_T I_a dI_f + K_T I_f dI_a = 0 \tag{9}$$

or $\left[\frac{dI_a}{dI_f}\right] = - \left[\frac{I_f}{I_a}\right]$

From Eqs.8 and 9, one obtains:

$$\left[\frac{I_a}{I_f}\right]^2 = \left[\frac{K_f(N_o)}{K_a}\right]$$

Then: $\left[\frac{I_a}{I_f}\right] = \left[\frac{K_f(N_o)}{K_a}\right]^{1/2} = k(N_o) \tag{10}$
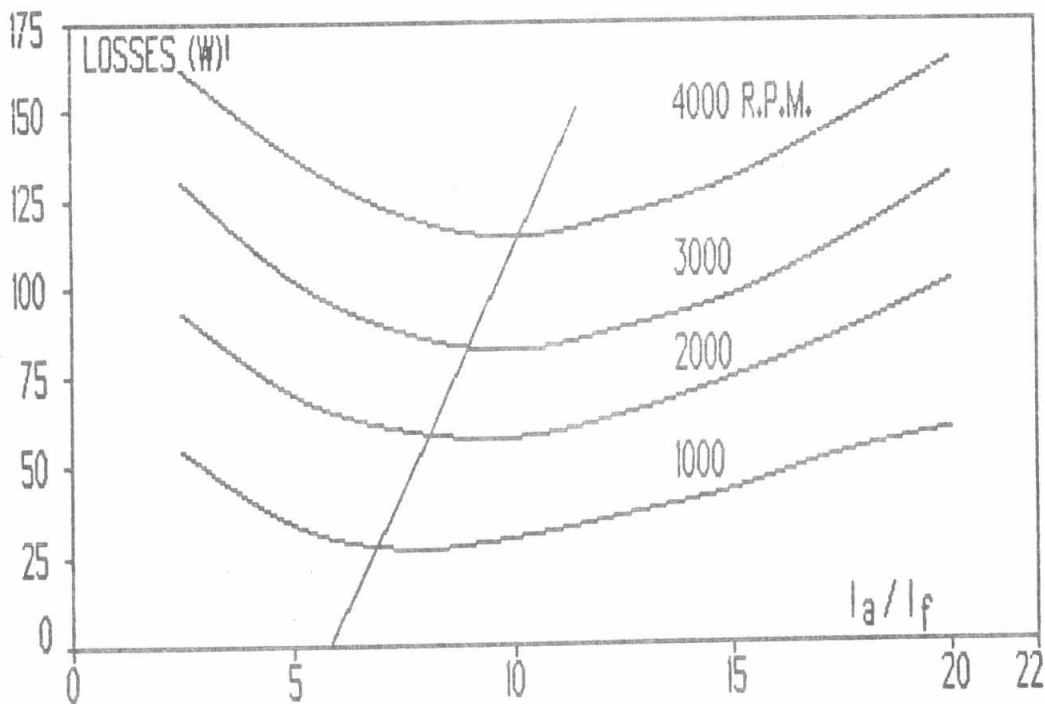


Fig.2 Evaluation of the Speed Constant k(N)

The optimal current ratio k(N) defined by Eq.10 is not easy to be obtained by measuring $K_f$ and $K_a$ due to the practical difficulties in separation of armature and field losses with the available test equipments. Instead the motor is tested at a light load where the total input power is only sufficient to cover the total losses. These losses are measured at variable $I_a/I_f$ ratio and constant speed. The results are plotted in Fig.2 at four constant speeds: 1000, 2000, 3000 and 4000 rpm where each graph has a

minimum losses point. From these graphs the following values of k(N) are obtained:

| | | | |
|---|---|---|---|
| k(N1) | = 0.78 | = $00.C8_{16}$ | at speed 1000 rpm. |
| k(N2) | = 0.91 | = $00.E9_{16}$ | 2000 rpm. |
| k(N3) | = 1.05 | = $01.0D_{16}$ | 3000 rpm. |
| k(N4) | = 1.12 | = $01.1F_{16}$ | 4000 rpm. |

These values of k(N) are represented internally in the MPU look-up table.

### B. Control System Structure:

The control system depicted in Fig.3 consists of three loops; one outer speed loop, and an inner armature current loop and a field current loop.
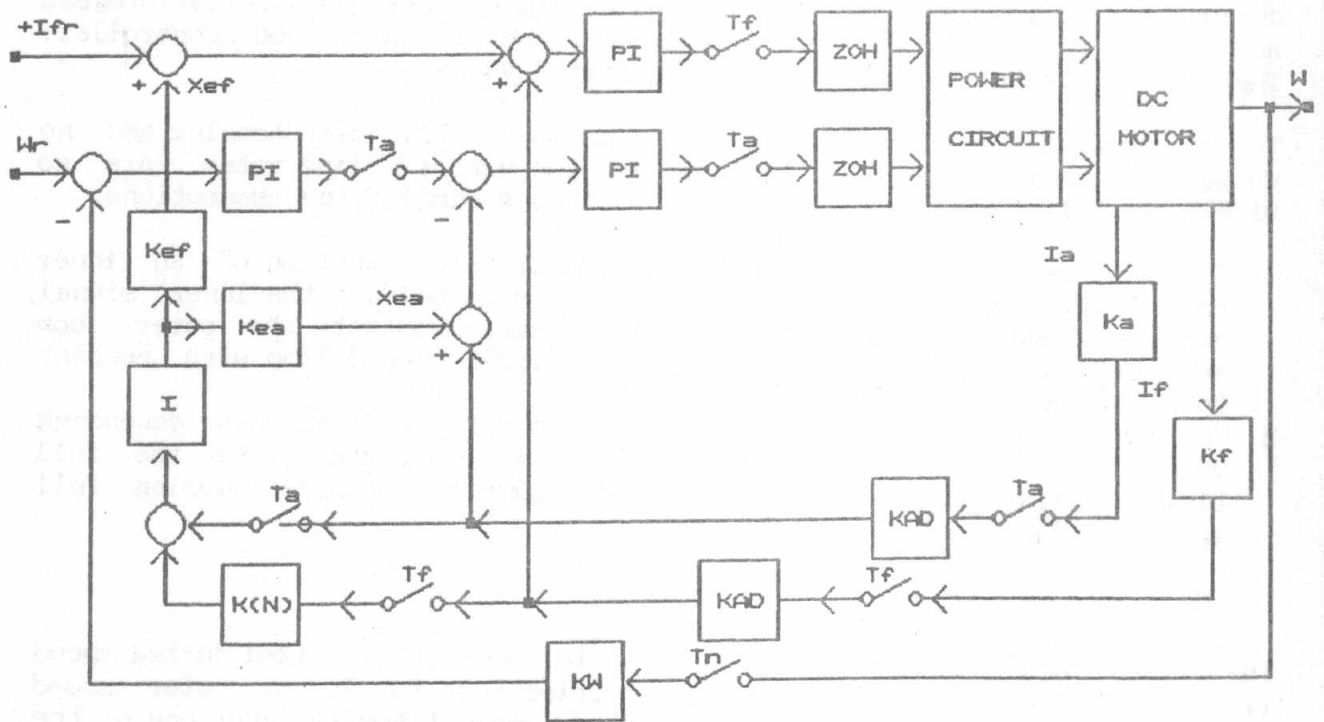


Fig.3 Structure of the Control System

As shown, the control system contains an error term of the current ratio in the form;

$$e_{eff} = I_a - k(N_o)I_f \tag{11}$$

This error is subjected to an integral correction and is used to adjust $I_a$ and $I_f$ to optimize the efficiency. Therefore at steady state this error term becomes zero and optimal efficiency is obtained.

The band-widths of the three control loops are widely different. The highest

frequency signal will determine the sampling frequency. Then to satisfy the sampling theory [5], the sampling period must be smaller than $T_a/2$. With microprocessors of limited computing power as the used M6800 this sampling period is very small to implement the controllers programs and the associated input/output operations.

In the present system, according to its parameters, there are three sampling rates; the armature current is sampled with a sampling period $T_a=1.178$ ms, the field current with a sampling period $T_f=8.245$ ms and the speed with a sampling period $T_n=24.736$ ms. The speed sampling period is dictated by the speed transducer, it is considerably smaller than the mechanical time constant ($\tau_m = 1s$). This is important from point of view of stability of the control system. The sampling periods $T_f$ and $T_a$ are selected also to be sufficiently smaller than $\tau_f$ and $\tau_a$ respectively and at the same time to be integral divisors of $T_n$ ($T_f=T_n/3$ and $T_a=T_n/21$). This is necessary so that synchronization of different samplers can be possible.

The armature sampling period $T_a$ is the smallest unit of time in the system, during this period the MPU executes the armature current controller program and parts of the field current controller and of the speed controller. Therefore $T_a$ cannot be smaller than the stated value.

The analysis of a multirate digital systems is usually quite complex and no unique approach can be used. Fortunately, the used sampling rates are so widely apart that we can introduce the following simplifying assumptions;

1. In analyzing the outer slower loop, the transfer function of an inner faster loop can be taken as a constant. This is because the inner signal reaches steady state in short period in comparison with the outer loop sampling period. This is true when the analyzing speed loop with respect to field and armature circuits.
2. Concerning the inner armature current loop, the coefficients depending upon field current ($K_e$ and $K_T$) are taken as constants during the full field sampling period. Also the speed is taken as a constant during full speed sampling period.

### C. Transient Response

The control system is designed such that field current is fixed during speed transients, thus control system is simplified into two loops; outer speed loop and inner armature current loop. The s-domain transfer functions of the speed (W) and armature current ($I_a$) are obtained. At a constant field current the following equations are given:

$$v_a(t) = E + i_a(t)R_a + L_a \left[ \frac{di_a(t)}{dt} \right] \tag{12}$$

$$K_T i_a = J \left[ \frac{dW}{dt} \right] + F \times W \tag{13}$$

Using these two equations, the block diagram in Fig.4.a is obtained. This can be simplified into the block diagram in Fig.4.b where;

$$G1(s) = \left[ \frac{sJ + F}{s^2 L_a J + s(R_a J + L_a F) + (R_a F + K_T K_E)} \right]$$

$$= \left[\frac{1}{L_a}\right] X \left[\frac{s + (F/J)}{s^2 + s(1/t_m + 1/t_a) + (1/t_m t_a + K_E K_T/L_a J)}\right] \quad (14)$$

$$G2(s) = \left[\frac{K_T}{sJ + F}\right] = \left[\frac{K_T/J}{s + 1/t_m}\right] \quad (15)$$

where:  $R_a = 0.3$ Ohm          $L_a = 0.81$ mH

$F = 8 \times 10^{-4}$ Nm/rad.s$^{-1}$     $J = 8 \times 10^{-4}$ kg.m$^2$

$K_T = 0.02$ Nm/A          $K_E = 0.02$ V/rad.s$^{-1}$

(At shunt field current = 1.8 A)

$\tau_a = L_a/R_a = 2.7$ ms  armature circuit time constant.
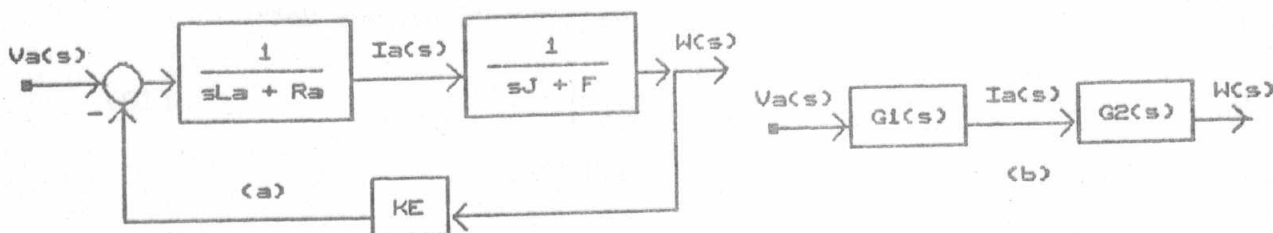
$\tau_m = J/F = 1.0$ s  mechanical time constant.



Fig.4 The Armature Controlled DC Drive

## III. THE DIGITAL CONTROLLERS

The analysis of the control system will be carried out using the z-transform which is the suitable approach in such digital control system.

### A. The armature Current Controller

The microprocessor control system executes a PI correction on the current error $e_a$ such that the armature current $I_a$ follows the reference armature current $I_{ra}$ with zero steady state error. The control algorithm also limits the value of $I_a$ to protect power circuit from over current at abrupt speed variations. In the transient periods this controller has only the single input $I_a$, but at steady state when efficiency optimization loop is in operation another input $(X_a)$ is presented as shown in Fig.5. The MPU implements the PI controller $G_c(z)$ numerically as:

$$G_c(z) = K_p + \left[\frac{K_i T_i z}{z - 1}\right] = K_d \left[\frac{z - z_d}{z - 1}\right] \quad (16)$$

where:  $K_d = K_p + K_i T_i$  and  $z_d = K_p/K_d$ \quad (17)

From the block-diagram of the armature current controller shown in Fig.5, the closed loop transfer-function is obtain in the following form:

$$G_a(z) = Z\left[\frac{1 - e^{-sTa}}{s} G_1(s)\right] = (1 - z^{-1}) Z\left[G_1(s)/s\right]$$

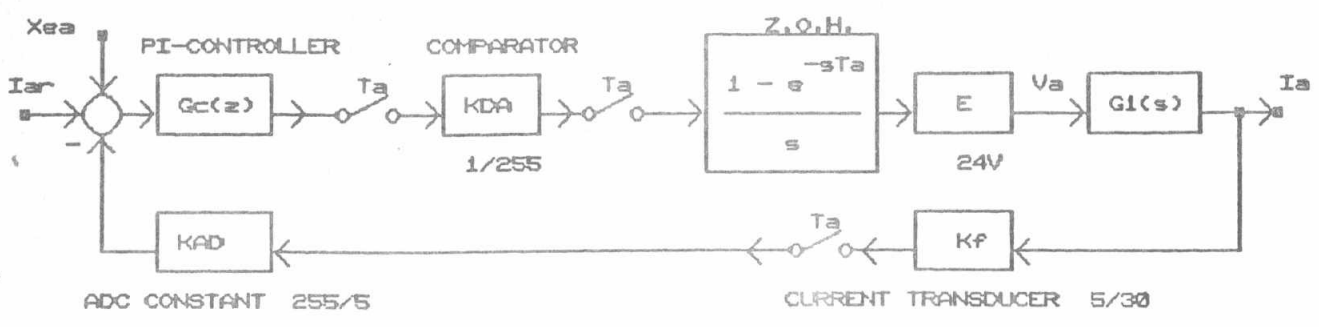$$G_a(z) = K_{aa}\left[\frac{z - z_1}{(z - p_1)(z - p_2)}\right] \quad (18)$$

Fig.5 The Block Diagram of the Armature Current Controller

Substituting numerical values and taking the z-transform one get:

$$G_a(z) = 1.1784 \left[ \frac{z - 0.9989}{( z - 368.7)( z - 2.68)} \right] \qquad (19)$$

The closed loop transfer function, $G_a(z)$ will be:

$$C_a(z) = \left[ \frac{K_{AD}\ E\ G_C(z)\ G(z)}{1 + K_{DA}\ K_f\ K_{AD}\ E\ G_C(z)\ G(z)} \right] \qquad (20)$$

$$= K_a \cdot \left[ \frac{z^2 - (z_d + z_1)z - z^1 \cdot z_d}{A3\ z^3 + A2\ z^2 + A1\ z + A0} \right] \qquad (21)$$

where:     $A3 = 1$                     $A2 = -K_1 + K_2 \cdot K_{da}$

$A1 = K_3 - K_2 \cdot (z_1 - z_{da}) \cdot K_{da}$     $A0 = -K_4 + z_{da} \cdot K_{da}$

Applying Jury's conditions of stability to characteristic Eq.20, then:

1. $F(1) > 0$     then     $A3 + A2 + A1 + A0 > 0$

    this gives:           $K_{da}( 1 - z_{da} ) > 0$ $\qquad (22)$

2. $F(-1) < 0$     then     $-A3 + A2 - A1 + A0 < 0$

    This gives           $K_{da} + K_{da} \cdot z_{da} < \ldots \ldots$ $\qquad (23)$

3. $|A0| < A3$

    this gives:           $\ldots \ldots < K_{da} \cdot z_{da} < \ldots \ldots$ $\qquad (24)$

4. $| A0^2 - A3^2| > ( A0\ A2 - A3\ A1 )$ $\qquad (25)$

Equations 22 through 25 give the boundary of $K_{pa}$ and $K_{ia}$ that render  stable closed loop system.

   B. Speed Controller

The  mechanical time constant ($\tau_m = 1s$) of the system is very high  compared with  the  armature  time constant ($\tau_a = 2.7$ mS)  and  similarly  the  speed sampling  period  $T_n$  is very high in comparison to  the  armature  sampling period  $T_a$. Thus it is a reasonable assumption to take the armature  current controller  as a constant when analyzing the speed controller. In fact  this constant is the scaling factor of the armature current, that is an  armature current  of  30 A corresponding to the hexadecimal number FF ($255_{10}$). This armature transfer function in the present case is taken as 30/255. Thus  the speed control system is reduced into Fig.6, where:

$$D_n(z) = K_{pn} + K_{in}T_{ni} \left[\frac{z}{z - 1}\right] = K_{dn} \left[\frac{z - z_{dn}}{z - 1}\right] \tag{26}$$

where:    $K_{dn} = K_{pn} + K_{in}T_{in}$    and    $z_{dn} = K_{pn}/K_{dn}$

The z-transform of the forward path is obtained in the following:

$$G_n(z) = \left[\frac{30}{255}\right].G_n(z) \ (1 - z^{-1}) \ Z\left[\frac{G_2(s)}{s}\right] \tag{27}$$

or  $$G_n(z) = 0.719 \ K_{dn} \left[\frac{z - z_{dn}}{(z - 1)(z - 0.9756)}\right] \tag{28}$$

The closed loop transfer function $C_n(z)$ is obtained as:

$$C_n(z) = \left[\frac{G_n(z)}{1 - G_n(z)K_n}\right] \tag{29}$$

$$C_n(z) = \left[\frac{0.719 \ K_{dn} \ ( \ z - z_{dn} \ )}{z^2 - (1.9756 - 0.0719 \ K_{dn})z + 0.9756 - 0.0719 \ K_{dn}z_{dn}}\right] \tag{30}$$

Applying Jury's stability conditions to the characteristic equation we obtain the following boundary of $K_{pn}$ and $K_{in}T_{in}$ to obtain a stable closed loop system:

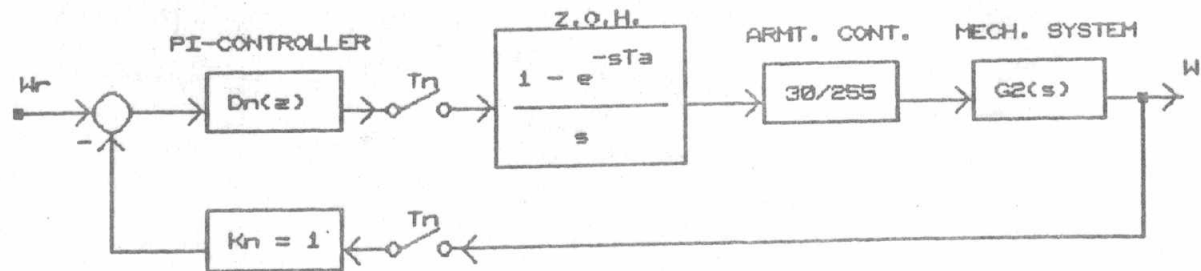$$27.06 > K_{pn} > 0.3394 \qquad \text{and} \qquad 2K_{pn} + K_{in}T_n > 54.95 \tag{31}$$



Fig.6 The Speed Controller

Measurement of the Actual Speed (Fig.7)

In the present work the speed is measured by a digital speed transducer as shown in Fig.7. It depends on an optical pulse tachogenerator having a slotted disk coupled with the motor shaft. The tacho-pulses are counted over a sampling period $T_n$=24.736 ms. The slotted disc has 127 slots on its periphery, and two opto-interrupters are used to the double number of pulses per revolution. The speed sampling time $T_n$ is calculated such that, count expresses the speed in rad/s. Thus if the number accumulated in speed counter at end of sampling period $T_n$ is N the following relation can be written:

$$N = \frac{W \times T_n \times (127 \times 2)}{2 \times 3.1416} \tag{32}$$

If N = W, then;

$$T_n = \frac{2 \times 3.1416}{2 \times 127} = 24.736 \times 10^{-3} \qquad (33)$$
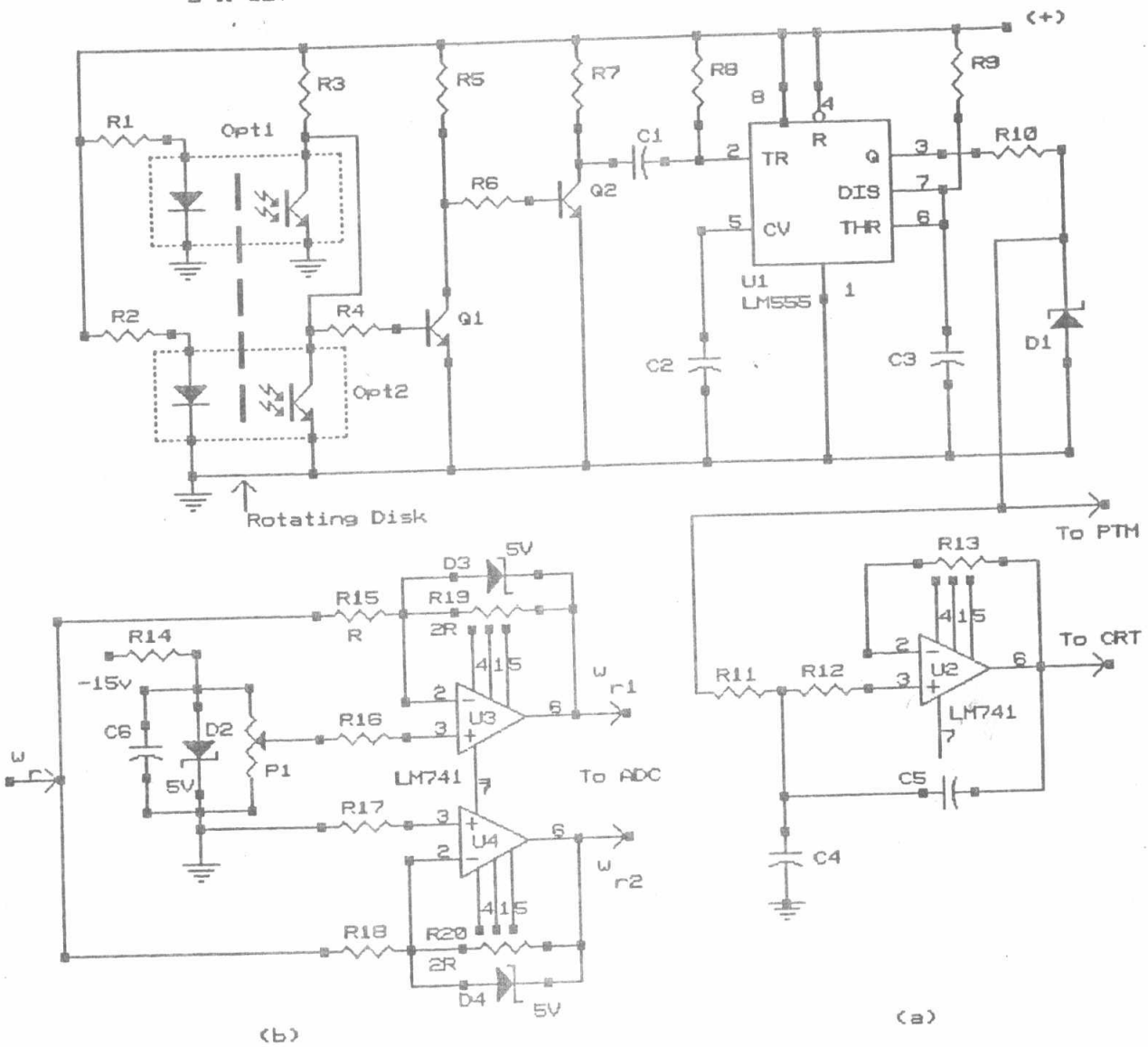


Fig.7 The Speed Measurement

## Measuring of the Reference Speed

In present application speed reference is entered via the ADC as an analog signal. The drawback of this method is that the speed measurement resolution can be limited to 1/256 which is the usual resolution of an 8-bit ADC. The circuit shown in Fig.7 together with the software used in Part II of this article improves this resolution to 1/512. The MPU reads the two signals W1 and W2 then it adds the two digital values to obtain the reference speed as a 9-bit number.

## C. The Field Controller

The field controller operates independently of the other controllers before abrupting speed transients to set the field current to a value suitable to

such transients. Apart from the speed transients the field controller operates normally to adjust the field current to a value which optimize the efficiency, by adding the input $X_{ef}$ to $I_{fr}$ as shown in the control block

diagram of Fig.1. It is to be noted that $I_{fr}$ is a constant predetermined value and not an output of the speed controller as $I_{ar}$. The block diagram of the field current controller is shown in Fig.8 where:

$$D_f(z) = K_{pf} + K_{if}T_f \left[\frac{z}{z-1}\right] = K_{df}\left[\frac{z - z_{df}}{z-1}\right] \tag{33}$$

Although the field power circuit is designed with a current rating equal to that of the series field current winding, instead of the shunt field winding, the total losses of field circuit is greatly reduced and it is found practically that the speed of response in the two cases is comparable.
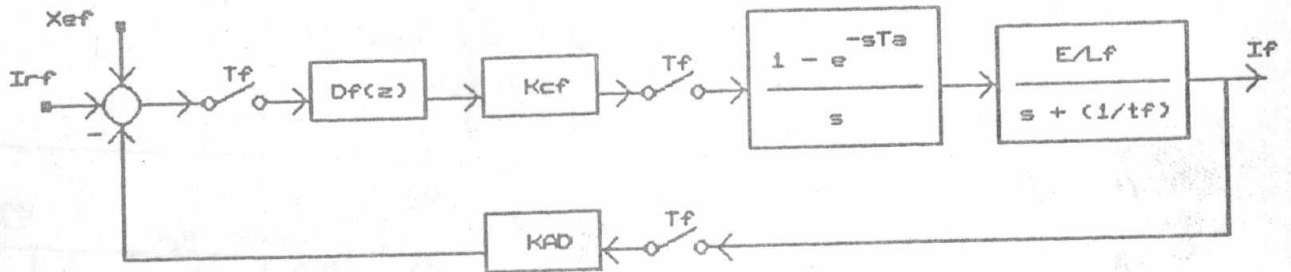


Fig.8 The Field Controller

Substituting the numerical values of field circuit $R_f = 6.7 \ \Omega$, $L_f = 0.268$ H, and $\tau_f = 40$ ms, the closed loop transfer function can be expressed as:

$$C_f(z) = A_f \left[\frac{z - z_{df}}{A_{2f}z^2 + A_{1f}z + A_{0f}}\right] \tag{34}$$

where: $A_f = K_{Cf} K_{df} \left[\frac{E}{R_f}\right].\left[1 - e^{-Tf/tf}\right]$ ; $A_{2f} = 1$

$A_{1f} = K_{ADf}K_{Cf}K_{DF} \left[\frac{E}{R_f}\right].\left[1 - e^{-Tf/tf}\right] - (1 + e^{-Tf/tf})$

$= 2.2243 \times 10^{-3}K_{df} - 1.8137$

$A_{0f} = -K_{Cf} K_{df} \left[\frac{E}{R_f}\right].\left[1 - e^{-Tf/tf}\right] + (1 + e^{-Tf/tf})$

$= -1.1121 \times 10^{-3}K_{df}z_{df} + 0.81372$

The stability boundary is :

$0 < K_{df} < 2530$ : $K_{df} - K_{df}z_{df} > 0$

$K_{df} + K_{df}z_{df} < 3268$ These are reduced into:

$0 < K_{pf} < 1634$ and $K_{if}T_f > 0$

The Measurement of the Currents

The armature current is measured, as shown in Fig.1, by sensing the voltage drop across a .02 Ω shunt in series with negative terminal of armature power circuit. The voltage appearing across shunt can be expressed as;

$$V_{shunt} = I_a \times R_{shunt} \times D_a \tag{34}$$
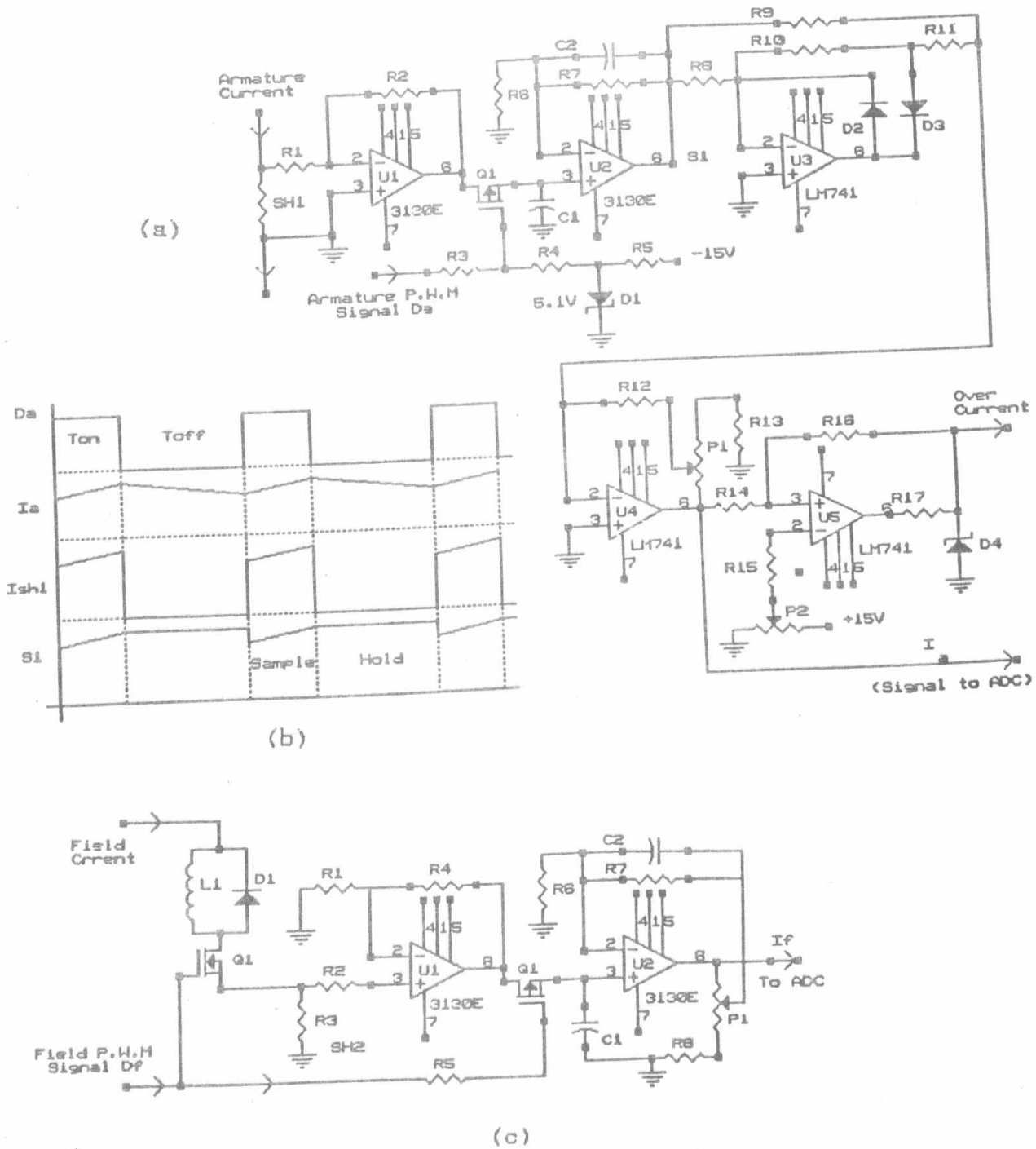


(a)

(b)

(c)

Fig.9 The Current Measurement

The analog switch Q1 in Fig.9.a, together with the operational amplifier U2 act as a Sample and Hold circuit, during the ON period Q1 is closed and the circuit output is proportional to $I_a$, during Off period Q1 (Fig.9.b) is opened holding the output at constant value till the next cycle. Since the chopper frequency is considerably high (31.125kHz),the armature leakage reactance greatly reduces the ripples in the current. The armature current measuring circuit gives the absolute value of current whatever its sign is. The comparator U5 is used to check if the armature current exceeds limit. Output of this comparator is connected to control system such that it generates a NMI to tell the MPU to take protective steps against the over current condition. The field current measuring circuit uses the same principle explained above, and it is shown in Fig.9.c.

## IV. EXPERIMENTAL RESULTS AND CONCLUSION

These will be given in the second part (Part II) of the study where the complete structures of the used Software and the Hardware are implemented and the whole system is tested.

### REFERENCES

[1] T. EGAMI, J. WANG & T. TSUCHIYA: "Efficiency Optimized Speed Control System, Synthesis Method Based On Improved Optimal Regulator Theory-Application to Separately Excited DC Motor System" , IEEE Trans. on I.E , Vol. IE-32, No.4 p.p 372-380, November 1985

[2] R. J. HILL: "Chopper Control of DC Disc-Armature Motor Using Power MOSFETs" .IEE PROC. March 1985, Vol.132.Pt. B.No.2, pp. 93-100 .

[3] B. S. DEWAN & A. MIRBOD: "Microprocessor-Based Optimum Control For Four-Quadrant Chopper", IEEE Trans. on I.A., Vol.IA-17, No. 1 pp. 34-40, Jan/Feb. 1981.

[4] R. Mostafa, Salah Gh. Ramadan and Gamal Sarhan: "Choppered DC Motor Drive using MOS and Bipolar Power Transistors"; 2nd Conference on Aeronautical Sciences and Aviation Technology, Military Technical College Cairo-Egypt 1987.

[5] B.C.KUO: "Digital Control Systems", HOLT, RINEHART & WINSTON Inc. 1980

[6] W.G.DUNFORD & S. B. DEWAN: "The Design of a Control Circuit of a Two Quadrant Chopper Based on the Motorola 6800 Microprocessor" IEEE Trans.on I.A.,VOL.IA-16,NO.4, pp. 495-500 ,JULY/AUGUST 1980

[7] B.J.CARDWELL, C.J.GOODMAN: "Response Improvements in Industrial DC Drives Driven From Optimal Analysis" IEE PROCEED, May 1984,Vol.131,Pt.B,N , p.p 91-99.

[8] R.R.SUL, B.J.VASANTH, T.KRISHNAN & M.KUMAR: "Microprocessor- Based Speed Control System for High-Accuracy Drives" IEEE Trnas. on I.E, VOL. IE-32 NO.3, pp.209-214, AUGUST 1985.

[9] J.B.PLANT, S.J.JORNA & Y.T.CHAN: "Microprocessor Control of Position or Speed of an SCR DC Motor Drive"IEEE Trnas. on I.E, VOL. IECI-27 NO.3, pp.228-234, AUGUST 1980

[10] M.R.STOJIC: "Design of the Microprocessor-Based Digital System for DC Motor Speed Control"IEEE Trnas. on I.E. VOL. IE-31 NO.3, pp.244-274, AUGUST 1985.

[11] A.K.LIN & W.W.KOESEL: "A Microprocessor Speed Control System" IEEE Trnas. on IECI, VOL. IECI-24 NO.3, pp.241-249, AUGUST 1977.

[12] Heath Company: "Individual Learning Program; MICROPROCESSORS" EE-3401 and ""Individual Learning Program; MICROPROCESSOR APPLICATIONS" ee-3405 Copyright (C) 1977, Heath Company U.S.A.